Title

Flavin Containing Monooxygenase 2 Prevents Cardiac Fibrosis via CYP2J3-SMURF2 Axis.

Authors

Ni, Cheng
Chen, Yongjian
Xu, Yinchuan
et al.

Publication Date

2022-07-05

DOI

10.1161/CIRCRESAHA.122.320538

Peer reviewed

HHS Public Access

Author manuscript

Circ Res. Author manuscript; available in PMC 2024 January 05.

Published in final edited form as:

Circ Res. ; : 101161CIRCRESAHA122320538. doi:10.1161/CIRCRESAHA.122.320538.

Flavin Containing Monooxygenase 2 Prevents Cardiac Fibrosis via CYP2J3-SMURF2 Axis

Cheng Ni, MD, PhD[a,†], **Yongjian Chen, PhD**[a,†], **Yinchuan Xu, MD, PhD**[a], **Jing Zhao, MSc**[a], **Qingju Li, MD, PhD**[a], **Changchen Xiao, MD, PhD**[a], **Yan Wu, MSc**[a], **Jingyi Wang, PhD**[a], **Yingchao Wang, MSc**[a], **Zhiwei Zhong, MSc**[a], **Ling Zhang, PhD**[a], **Rongrong Wu, PhD**[a], **Qingnian Liu, PhD**[a], **Xianpeng Wu, MD**[a], **Changle Ke, PhD**[a], **Wei Zhu, PhD**[a], **Jinghai Chen, PhD**[a], **Jijun Huang, Ph.D**[b], **Yibin Wang, PhD**[c], **Jian'an Wang, MD, PhD**[a], **Xinyang Hu, PhD**[a,*]

[a]Department of Cardiology, Cardiovascular Key Lab of Zhejiang Province, The Second Affiliated Hospital, College of Medicine, Zhejiang University, Hangzhou 310009, P.R. China

[b]Division of Molecular Medicine, Department of Anesthesiology, David Geffen School of Medicine, University of California at Los Angeles (UCLA), Los Angeles, California, USA.

[c]Programme in Cardiovascular and Metabolic Diseases, Duke-NUS Medical School, 8 College Road, Singapore

Abstract

Background: Cardiac fibrosis is a common pathological feature associated with adverse clinical outcome in post-injury remodeling, and has no effective therapy. Using an unbiased transcriptome analysis, we identified Flavin-Containing Monooxygenase 2 (FMO2) as a top-ranked gene dynamically expressed following myocardial infarction (MI) in hearts across different species including rodents, non-human primates and human. However, the functional role of FMO2 in cardiac remodeling is largely unknown.

Methods: Single nuclear transcriptome analysis were performed to identify FMO2 after myocardial infarction, FMO2 ablation rats were generated both in genetic level using CRISPR-cas9 technology and lentiviral mediated manner. Gain of function experiments were conducted using *postn*-promoter FMO2, miR1a/miR133a-FMO2 lentivirus and enzymatic activity mutant FMO2 lentivirus after MI.

Results: A significant down-regulation of FMO2 was consistently observed in hearts after MI in rodents, non-human primate and patients. Single nuclei transcriptome analysis showed cardiac expression of FMO2 was enriched in fibroblasts rather than myocytes. Elevated spontaneous tissue fibrosis was observed in the FMO2-null animals without external stress. In contrast, fibroblast specific expression of FMO2 markedly reduced cardiac fibrosis following MI in rodents and non-human primates associated with diminished SMAD2/3 phosphorylation. Unexpectedly, the FMO2 mediated regulation in fibrosis and SMAD2/3 signaling was independent of its enzymatic activity.

[*]**Address correspondence to:** Xinyang Hu, PhD, Department of Cardiology, Cardiovascular Key Lab of Zhejiang Province, Department of Cardiology, The Second Affiliated Hospital, College of Medicine, Zhejiang University, Hangzhou 310009, P.R. China, hxy0507@zju.edu.cn.

[†]These authors contribute equally to this study.

Disclosure: None.

Rather, FMO2 was detected to interact with cytochrome p450 superfamily 2J3 (CYP2J3). Binding of FMO2 to CYP2J3 disrupted CYP2J3 interaction with SMAD specific E3 ubiquitin ligase 2 (SMURF2) in cytosol, leading to increased cytoplasm to nuclear translocation of SMURF2 and consequent inhibition of SMAD2/3 signaling.

Conclusions: Loss of FMO2 is a conserved molecular signature in post-injury hearts. FMO2 possess a previously uncharacterized enzyme-independent anti-fibrosis activity via CYP2J3-SMURF2 axis. Restoring FMO2 expression exerts potent ameliorative effect against fibrotic remodeling in post-injury hearts from rodents to non-human primate. Therefore, FMO2 is a potential therapeutic target for treating cardiac fibrosis following injury.

Graphical Abstract

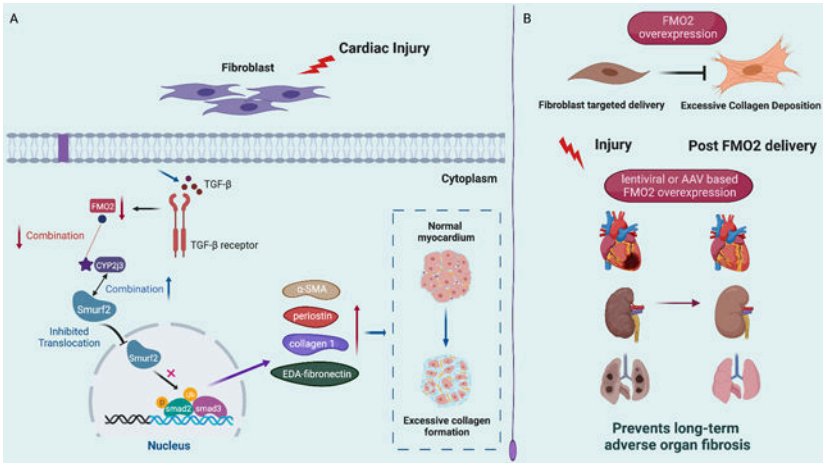

Subject Terms:

Myocardial Infarction; Remodeling; Flavin Containing Monooxygenase 2 (FMO2); Cardiac Fibrosis; Myocardial Infarction; Non-human primate

Introduction

Fibrosis is a common feature of cardiac pathological remodeling after injury and a major detriment to cardiac repair, regeneration and functional recovery. There is no effective treatment proven clinically to prevent tissue fibrosis. Progressive scaring remains to be one of the most challenging clinical issues underlying many chronic human heart diseases[1], including heart failure after myocardial infarction (MI)[2], dilated cardiomyopathy and hypertrophic cardiomyopathy associated with hypertension. This is also true for other organ pathologies including pulmonary, renal and dermal fibrosis[3–5]. Under normal condition, resident fibroblasts are quiescent and produce low levels of extracellular matrix (ECM) proteins[6,7]. Following acute injury or under chronic stress, however, fibroblasts are activated and play a dominant role in fibrotic remodeling. Fibroblast activation is characterized by elevated expression of contractile proteins, enhanced cell mobility, induction of pro-inflammatory genes, and high levels of deposition of collagens and other extra-cellular matrix proteins[8,9]. Transforming Growth Factor-β1(TGF-β1) [10,11] and its downstream SMAD2/3 phosphorylation [12,13] is the most important intracellular signaling

in fibroblast activation, including myofibroblast activation in heart. While fibrotic response can be protective during wound healing by preventing myocardial wall rupture, prolonged activation leads to excessive scarring and loss of tissue compliance as in the case of post-MI hearts[14–16]. Indeed, SMAD2/3 phosphorylation is persistently activated in the infarcted area during post-ischemic period. More importantly, this pro-fibrotic signal can expand from infarct zone to ischemic border area, and even penetrates into non-infarcted area, leading to progressive remodeling and functional deterioration. So far, no effective remedy is available to effectively block TGF-β downstream signaling in order to attenuate fibrotic progression in post injury heart.

In the current study, we performed an unbiased transcriptome analysis in post-myocardial infarcted hearts. Flavin-Containing Monooxygenase 2 (FMO2) expression was found to be one of the top ranked genes whose expression was dynamically correlated with the onset of cardiac-injury and fibrosis. Importantly, FMO2 was detected to be enriched in cardiac fibroblast but not in myocytes. Genetic inactivation of FMO2 gene in rats induced spontaneous fibrosis in heart. In contrast, FMO2 expression in cardiac fibroblasts significantly attenuated TGF-β induced myofibroblast activation and SMAD2/3 phosphorylation. Mechanistically, we established that FMO2 expression negatively regulated TGF-β signaling in an enzymatic activity-independent manner by promoting the expression and nuclear translocation of SMAD Ubiquitination Regulatory Factor 2 (SMURF2), an intrinsic negative regulator of SMAD2/3 phosphorylation and TGF-β1 signaling. Finally, ectopic expression of FMO2 prevented fibrosis and attenuated post-MI remodeling and dysfunction in heart in rodent and non-human primates. Therefore, our study revealed FMO2 as a previously uncharacterized intrinsic inhibitor of TGF-β/SMAD2/3 signaling with conserved ameliorative effect on cardiac fibrosis and pathological remodeling. Restoring FMO2 expression via targeted gene delivery could be a new therapeutic approach in treating cardiac fibrosis.

Methods

The detailed methods are described in online Data Supplement. Please see also the Major Resources Table in the Supplemental Data for details of the reagents and models.

Data Availability

All key data supporting the conclusion are presented in main figures, table or supplemental figures and supplemental tables. Additional methods or data related to this study are available from the corresponding authors upon reasonable request.

Results:

Dynamic expression of FMO2 following cardiac injury

To uncover the relevant genes involved in cardiac remodeling following myocardial infarction (MI), we performed unbiased transcriptomic analysis in the infarcted and peri-infarct ventricular tissue obtained from sham operated and post-MI rats. Among the genes significantly down-regulated in the post-MI heart (133 genes in total, fold change>2, $p<0.05$) (Supplemental Figure 1A), Flavin Containing Monooxygenase 2 (FMO2), Aldehyde

dehydrogenase family 5 member A1 (Aldh5a1) and 15 Lipoxygenase 1 (ALOX15) were ranked on the top based on fold of changes. However, only FMO2 demonstrated similar changes at protein level in the post-MI rat heart tissue (Figure 1A–1B). In contrast, the protein levels of ALOX15 and Aldh5a1 were not observed to be statistically different after MI (Supplemental Figure 1B). FMO2 is a member of the FMO family which includes five isoforms (FMO1–5). Unlike other isoforms which are highly expressed in liver, FMO2 mRNA is predominantly expressed in lung but also detected at substantial levels in other organs, including heart (Supplemental Figure 1C). In heart, FMO2 expression was most abundantly detected in cardiac fibroblasts and endothelial cells, but not in myocytes, based on immunostaining in adult heart section, western blotting from primary neonatal rat ventricular myocytes vs. fibroblast and single-nuclei RNA sequencing analysis (Figure 1C–1F, Supplemental Figure 1D–1E). Importantly, in addition to rat, the post-MI down-regulation of cardiac FMO2 expression was also observed in mice (Figure 1G–1H) and non-human primates (Figure 1I–1J). Hence, loss of FMO2 expression appears to be a conserved molecular signature in association with post-injury remodeling and fibrosis across multiple mammalian species.

Loss of FMO2 is sufficient to promote cardiac fibrosis and dysfunction

To demonstrate the functional significance of FMO2 down-regulation, we performed intramyocardial injection of a lentivirus harboring FMO2 shRNA (LV-shFMO2, 1*10^8 pfu/animal) in rat left ventricular wall. The efficacy of the shRNA mediated FMO2 inactivation was validated at protein level by immunoblot (Figure 2A). A notable reduction in cardiac performance was detected in the FMO2 shRNA treated hearts comparing to the controls at 2 weeks post-injection based on echocardiographic parameters, including reduced ejection fraction (EF) and dilated cardiac internal dimension at both systolic and diastolic phases. The observed defects in cardiac function persisted at one-month post FMO2 inactivation (Figure 2B–2C, Supplemental Figure 2A–2C, Supplemental Table 1). More importantly, we discovered a significant deterioration in diastolic function in the FMO2 KD heart as indicated by altered E/A and E/E’ (Supplemental Figure 2D–2E). Consistent with echocardiogram results, hemodynamics data also revealed deteriorated cardiac systolic and diastolic function when FMO2 was silenced (Supplemental Figure 2F–2I). In addition, we observed significantly increased expression of fibrotic genes, accompanied by elevated phosphorylation of SMAD2/3 in FMO2 KD hearts (Figure 2D–2G). Histological analysis detected a marked increase in interstitial fibrosis within the ventricular myocardium (Figure 2H–2I) in the FMO2 KD hearts compared to controls. Significant trans-differentiation of fibroblast to myofibroblast was observed in the FMO2 knock-down heart as demonstrated by the induced expression of marker genes, α-SMA and S100A4 (Figure 2J–2K).

To further demonstrate the role of FMO2 in cardiac fibrosis and remodeling, we generated a FMO2-null rat by CRISPR-cas9 mediated genome editing (Supplemental Figure 2J–2K). Serial echocardiography in the FMO2−/− rats detected diastolic dysfunction characterized by abnormal E/A ratio accompanied with impaired E/E’ ratio beginning at 12 to 16 weeks of age (Supplemental Figure 2L–2M), followed by progressive reduction of ejection fraction and chamber dilation (Figure 2L–2M, Supplemental Figure 2N–2O, Supplemental Table 2). Again, wide-spread interstitial fibrosis was detected in the FMO2−/− ventricular

myocardium at 16 weeks of age without external stress (Figure 2N–2O). In the meanwhile, the expression levels of fibrotic markers, including α-SMA, collagen1, EDA-fibronectin, and periostin, were significantly elevated in the FMO2−/− hearts (Figure 2P–2Q), also accompanied by elevated phosphorylation of SMAD2/3 (Figure 2R–2S).

Expression of FMO2 in cardiac fibroblast prevents cardiac fibrosis and preserves cardiac function after MI

To further demonstrate the functional impact of FMO2 expression *in vivo*, we injected an FMO2 expressing lentivirus (LV-FMO2, 1*10^8 pfu/animal) in rat hearts at 5 separate points around the border zone immediately following MI (Supplemental Figure 3A). Restoration of FMO2 expression was observed from day 7 post MI, and persisted at a significant level at day 28 after MI (Supplemental Figure 3B) without a significant impact on the expression of other FMO family members (Supplemental Figure 3C–3F). Cardiac output was significantly improved while pathological remodeling was ameliorated as indicated by preserved ejection fraction and attenuated chamber dilation in the FMO2 treated hearts at Day28 post MI, comparing to the untreated hearts (Supplemental Figure 3G–3K, Supplemental Table 3). Scar sizes were markedly reduced (Supplemental Figure 3L–3M) and interstitial fibrosis levels were reduced in the non-infarcted areas (Supplemental Figure 3N–3O), along with dramatically down-regulated expression of Periostin (Supplemental Figure 3P). Therefore, restoration of FMO2 expression in cardiac fibroblast dramatically decreased cardiac fibrosis and pathological remodeling, and significantly preserved cardiac function following MI.

We have showed previously that endogenous FMO2 was highly enriched in non-myocytes in rodent hearts. To determine whether FMO2 mediated cardio-protection *in vivo* was contributed by cardiomyocytes vs. non-cardiomyocytes, we constructed an expression cassette where 2 tandem copies of the 22-bp complementary target sequence for cardiac specific mir-1a-3p and mir-133a-3p were added at the 3′ end of the FMO2 cDNA (LV-miR133a/1a TS FMO2, referred to as LV-nmFMO2). Consistent with the previous report [17], this strategy restricted the FMO2 transgene expression only in the non-myocytes following intramyocardial injection (Supplemental Figure 4A–4D). Using the same treatment scheme as for the LV-FMO2 vector (Figure 3A), expression of FMO2 in non-myocytes also significantly improved post-MI cardiac function compared to the control treated cohort (Figure 3B–3C, Supplemental Figure 4E–4G, Supplemental Table 4). It was noted, however, the impact on diastolic parameters was minimal (Supplemental Figure 4H). In addition, nonmyocyte targeted expression of FMO2 also reduced scar circumference compared with the controls (Figure 3D–3E), significantly diminished interstitial fibrosis in the non-infarcted area (Figure 3F–3G) along with reduced expression of fibrotic marker gene Periostin (Supplemental Figure 4I). Importantly, restoring non-myocyte FMO2 expression using a lentiviral vector (LV-nmFMO2) in the $FMO2^{-/-}$ rats significantly improved systolic function (Supplemental Figure 5A–5E, Supplemental Table 5) along with reduced fibrosis (Supplemental Figure 5F–5G) and collagen deposition (Supplemental Figure 5H). Thus, these *in vivo* data indicate that loss of FMO2 expression is sufficient to promote widespread cardiac fibrosis and progressive dysfunction without external stresses.

To further support the cell specificity of FMO2 mediated anti-fibrosis effect, we generated a FMO2 lentivirus using Periostin-promoter to target FMO2 expression in periostin positive myofibroblast (*Postn*-promoter FMO2) as shown via immunofluorescent microscopy (Supplemental Figure 6A). In parallel, we isolated cardiac fibroblast, cardiomyocyte and endothelial cells respectively from *Postn*-promoter FMO2 injected MI rat (28days after MI). As measured by anti-FLAG antibody, we detected significant FMO2-FLAG protein in periostin positive myofibroblast, but nearly no signals in cardiomyocytes and endothelial cells (Supplemental Figure 6B). In the post-MI hearts treated with *Postn*-FMO2-Flag lentivirus, myofibroblast specific FMO2 expression was detected only after Day 7 post-injection (the same as LV-FMO2 experiment) but persisted at Day 28, and resulted in significantly improved cardiac function at Day 28 after MI (Figure 3H–3J, Supplemental Figure 6C–6E, Supplemental Table 6). In contrast, the reparative fibroblast proliferation in the infarcted area was not affected in acute phases at Day 3 post-MI (Supplemental Figure 6F–6G). At Day 28 post-MI, scar sizes were reduced and pro-fibrotic protein expression was lowered by *postn*-FMO2-FLAG treatment (Figure 3K–3L, Supplemental Figure 6H). Importantly, fibrosis in non-infarcted area was also significantly decreased following FMO2 expression in myofibroblasts (Figure 3M–3N).

FMO2 belongs to a family of genes with known enzymatic activity for NADPH-dependent N-oxidation of primary alkylamines. To determine whether the enzymatic activity of FMO2 is involved in fibrosis regulation, we generated a lentivirus expressing enzymatic deficient FMO2 mutant (LV-FMO2mut) with deletion of the amino acid residues known to be necessary for NADP or FAD binding (aa9–13, aa40–41, aa60–62, aa195–198) (LV-FMO2mut). Unexpected, similar to the protective effect observed for the wildtype full-length FMO2, the LV-FMO2mut injection also significantly improved cardiac function (Supplemental Figure 7A–7E, Supplemental Table 7), along with decreased fibrotic area (Supplemental Figure 7F–7G) and fibrotic protein expression (Supplemental Figure 7H). These *in vivo* evidence suggest that loss of FMO2 expression in post-MI heart is a significant contributor to fibrosis induction and dysfunction, and restoring FMO2 expression in myofibroblast has potent anti-fibrotic effects in post-injury heart in an enzymatic activity independent manner.

Anti-fibrotic activity of FMO2 in non-human primates

We have demonstrated that loss of FMO2 expression in post-MI heart is a conserved molecular signature from rodents to non-human primates. In order to validate the functional impact of FMO2 expression in a more translationally relevant monkey model, we generated a monkey specific lenti-viral vector for targeted expression of FMO2 in nonmyocytes (LV-miR133a/1a-TS-FMO2, or LV-MnmFMO2). A total of 2*10^9 particles per animal of LV-MnmFMO2 or control vector were delivered into the peri-infarct zone via 10 intra-myocardial injections following LAD ligation. Cardiac function was assessed by Cardiac Magnetic Resonance Imaging (CMR) and echocardiography. As shown in Figure 4A–4B and in 4E and Supplemental Table 8, a significant improvement in cardiac function was observed in the FMO2 treated group up to 4 weeks post-MI, accompanied by significantly attenuated left ventricle chamber dilation (Figure 4C–4D, 4F–4G and 4I), markedly reduced infarct sizes (Figure 4H–4K) and scar thickness based on both MASSON staining and

histological sections across the apex (Figure 4J, 4L–4M). Consistent with a reduced fibrosis, intra-cardiac collagen levels were significantly reduced in the post-MI monkey hearts receiving FMO2 treatment (Figure 4N–4O). Taken together, our data provide clear *in vivo* evidence to support a conserved anti-fibrotic and cardio-protective effect of FMO2 expression, and its potential as a therapeutic modality for post-MI pathological remodeling.

FMO2 antagonizes TGF-β induced fibroblast induction independent from its enzymatic activity

Our *in vivo* data implicated an anti-fibrosis effect from fibroblast specific FMO2 expression in heart. In primary neonatal rat cardiac fibroblast (NRCFs) cultured under basal conditions without TGF-β stimulation, minimal expression of fibrotic proteins and SMAD2/3 phosphorylation was observed. Treatment of a potent inhibitor for TGF-β receptor ALK5 (SB431542) showed no significant impact on the expression of fibrotic proteins or SMAD2/3 phosphorylation in the absence of external TGF-β stimulation, but effectively blocked their induction under TGF-β stimulation (Supplemental Figure 8A–8B). Therefore, NRCF in culture had minimal TGF-β autocrine activity at basal level, and could serve as an *in vitro* system to investigate TGF-β dependent signaling and fibrotic induction. In NRCF, FMO2 expression was dramatically down-regulated upon TGF-β stimulation at doses as low as 2 ng/ml, concurrent with a significant induction of fibrotic genes (Figure 5A). In contrast, over-expression of FMO2 significantly reduced TGF-β stimulated induction of pro-fibrotic genes (Supplemental Figure 8C–8D). In cardiac fibroblasts (CFs) isolated from the $FMO2^{-/-}$ rats, the expression of pro-fibrotic genes including periostin, α-SMA, vimentin, collagen1 and EDA-fibronectin was elevated even under basal conditions relative to the wildtype controls (Figure 5B–5C), consistent with the fibrotic basal phenotype observed in the $FMO2^{-/-}$ hearts. As expected, restoration of FMO2 expression in the $FMO2^{-/-}$ CFs potently repressed the induction of fibrotic genes in response to TGF-β stimulation (Figure 5D–5E). Notably, combination treatment of a TGF-β inhibitor, SB431542, and FMO2 expression did not show additive effects on suppressing fibrotic protein expression or SMAD2/3 phosphorylation under TGF-β stimulation (Supplemental Figure 8A–8B). In short, FMO2 expression potently suppresses TGF-β induced fibrotic gene activation and downstream signaling in cardiac fibroblasts.

Consistent with the observation made *in vivo*, expression of a FMO2 mutant without enzymatic activity using LV-FMO2 mut vector conferred comparable anti-fibrotic effect as expressing a wild type FMO2 (Figure 5F–5G, Supplemental Figure 8E). Intriguingly, a polymorphic allele of FMO2 has been reported in human and rat that expresses an enzymatic defective isoform with 64 amino-acid deletion at its C-terminus [18]. Indeed, we showed that the expression of this truncated isoform of human FMO2 in NRCF also conferred a similar inhibitory effect on TGF-β induced fibrotic genes and downstream signaling (Supplemental Figure 8F). All these data suggest that FMO2 is a potent inhibitor of TGF-β induced fibrotic induction independent of its monooxygenase activity.

FMO2 antagonizes TGF-β signaling via interacting with CYP2J3

To explore the molecular mechanism underlying this enzyme-independent but FMO2-dependent inhibition of TGF-β signaling, we examined the effects of FMO2 expression

on multiple intracellular signaling pathways downstream of TGF-β in cardiac fibroblasts. As shown in Figure 6A–6B, phosphorylation of SMAD2 at 465/467 and SMAD3 at 423/425 in TGF-β treated cardiac fibroblasts was significantly inhibited by FMO2 expression, while the phosphorylation levels of SMAD7, SMAD4 and SMAD3 (s204) were not affected. The other non-canonical TGF-β pathways, including ERK and p38 activities were not altered neither.

To understand how FMO2 protein regulates SMAD2/3 phosphorylation, we analyzed FMO2 interactome in cardiac fibroblast by immunoprecipitation followed up mass-spectrometry (Supplementary Figure 9A and detailed in Methods). Among the proteins detected in the FMO2 protein complex, Cytochrome P450 superfamily 2J3 (CYP2J3) showed the highest level of coverage (Supplementary Figure 9B). CYP2J3 is a member of the cytochrome P450 (CYP) epoxygenase gene family, known for its role in arachidonic acid metabolism. CYP2J3 and FMO2 were both detected in the same cellular fraction, enriched with microsome and endoplasmic reticulum (ER) (Supplementary Figure 9C). The interaction between FMO2 and CYP2J3 in NRCF was confirmed by reciprocal co-immunoprecipitation assays for the ectopically expressed tagged-proteins using in either anti-FMO2 or anti-CYP2J3 antibodies (Figure 6C–6D). However, these commercially available antibodies were not adequate in quality to allow us to perform reciprocal CO-IP for the endogenous proteins. Nevertheless, in NRCF, suppression of CYP2J3 by shRNA significantly blocked FMO2 mediated inhibition of SMAD2/3 phosphorylation and pro-fibrotic gene expression following TGF-β stimulation (Figure 6E–6H). Therefore, CYP2J3 is a potential interacting partner and a necessary downstream effector in FMO2 mediated inhibition of TGF-β signaling.

To further elucidate the molecular basis of FMO2-CYP2J3 interaction, we used a protein docking algorithm to predict the interaction sites between FMO2 and CYP2J3 based on available protein structures. In this docking model, the residues Gln169, Val180, Glu183 of FMO2 and the residues Lys478, Ser493 and His494 of CYP2J3 were found to be located at a potential binding interface between the two proteins (Supplementary Figure 9D). Targeted mutations of these putative interacting sites in either FMO2 (ΔFMO2) or CYP2J3 (ΔCYP2J3) abolished their interactions in cells, further supporting a direct interaction between the two proteins (Figure 6I–6J).

FMO2-CYP2J3 interaction promotes nuclear translocation of SMURF2 and inhibits SMAD2/3 phosphorylation

Since FMO2 and CYP2J3 are cytosolic located proteins and are unlikely involved directly in gene regulation at transcription level, we further investigated post-transcriptional role of FMO2 mediated inhibition of SMAD2/3 phosphorylation and the ensuing anti-fibrosis effect in heart. Indeed, we observed that inhibiting protein degradation by treating fibroblast with MG132, the FMO2 mediated inhibition of SMAD2/3 phosphorylation was markedly blocked while the total SMAD2/3 protein remained no statistically different (Figure 7A). This data suggests that phosphorylated SMAD2/3 was selectively degraded by FMO-CYP2J3 mediated activity via proteasome dependent manner. SMAD specific E3 ubiquitin ligase 2 (SMURF2) is an E3 ubiquitin ligase with specific activity towards phosphorylated SMAD2/3 in the nucleus [19], and has an demonstrated important role

in negative regulation of TGF-β signaling. Indeed, knocking-down SMURF2 in NRCF markedly blocked FMO2 mediated anti-TGF-β signaling and anti-fibrotic effects as measured by levels of phosphorylated SMAD2/3 and fibrotic gene expression (Figure 7B–7E). Interestingly, we detected a specific protein-protein interaction between CYP2J3 and SMURF2 using reciprocal co-immunoprecipitation assays (Figure 7F–7G). Importantly, FMO2 expression disrupted the interaction between CYP2J3 and SMURF2 in fibroblast (Figure 7H–7I) and promoted SMURF2 nuclear translocation. Furthermore, expression of the ΔFMO2 mutant with no binding activity to CYP2J3 did not reduce the interaction between SMURF2 with CYP2J3, nor promoting the nuclear translocation of SMURF2 (Figure 7J). Consequently, the expression of the ΔFMO2 mutant failed to suppress TGF-β induced downstream signaling and fibrotic gene expression in fibroblasts (Figure 7K–7L). These data demonstrate that FMO2 modulates CYP2J3-SMURF2 interaction through direct binding and ultimately promotes SMURF2 nuclear translocation to inhibit TGF-β signaling.

The conserved regulation and functions of FMO2 in human cardiac fibroblasts from MI patients

To validate the clinical relevance of FMO2-SMURF2 axis in TGF-β regulation, we collected LV free wall heart tissue samples from patients with acute MI or previous MI who were subjected to heart transplantation (scar area), as well as from patients died of non-cardiac sudden death or intracranial hemorrhage (LV free wall) as controls (Figure 8A). Consistent with the observations made in mouse, rat and non-human primate, the expression levels of FMO2 were significantly downregulated in the post-MI human hearts when compared to the non-MI control hearts (Figure 8B–8C, detailed patients baseline characteristics are provided in Supplemental Table 9). Moreover, re-expression of human FMO2 in human primary cardiac fibroblasts (Human CFs) isolated from the scar area of MI patient's hearts also significantly blunted the induction of pro-fibrotic genes (Figure 8D–8E), and TGF-β signaling, including SMAD2/3 phosphorylation (Figure 8F–8G). Consistent with these molecular changes, human cardiac fibroblast isolated from post-MI patients showed extended pseudopods and enlarged cell surface areas comparing to the fibroblasts isolated from normal hearts, and these changes were significantly repressed by FMO2 expression (Figure 8H). Therefore, expression of FMO2 in human cardiac fibroblasts from post-MI hearts suppressed pro-fibrotic signaling and fibrotic gene expression as in rodent and non-human primates. Thus, restoration of FMO2 in cardiac fibroblasts of MI patients represents a promising therapeutic intervention to treat cardiac fibrosis.

FMO2 expression prevents multiple forms of organ fibrosis

FMO2 and its downstream effectors CYP2J3/SMURF2 are ubiquitously expressed across different organs and tissues. We indeed observed that the basal fibrosis levels in the FMO2−/− rats were also significantly elevated in lung and kidney (Supplemental Figure 10A–10B). Consistent with these histopathological evidences, collagen levels, as determined by immunoblot, were also significantly increased in both lung and kidney in the FMO2−/− rats (Supplemental Figure 10C–10F). Based on the protective outcomes observed in heart, we then examined the effect of FMO2 expression in pulmonary fibrosis induced by trachea administration of Bleomycin. Remarkably, using an AAV6-FMO2 vector which showed a preferred target specificity to lung tissue (Supplemental Figure 11A–11B, Supplemental

Figure 12A), FMO2 expression mitigated the severity of pulmonary fibrosis induced by Bleomycin as demonstrated by reduced hydroxyproline content (Supplemental Figure 12B) and MASSON staining signal (p=0.0501) (Supplemental Figure 12C–12D). Similarly, we detected that FMO2 expression was significantly down-regulated in fibrotic kidney induced by unilateral ureter obstruction procedure (UUO) in rats (Supplemental Figure 11C–11D). Remarkably, delivery of FMO2 expressing lentiviral vector (LV-FMO2) via distal kidney vein administration significantly ameliorated nephron remodeling following UUO surgery as demonstrated by H/E staining and MASSON trichrome staining (Supplemental Figure 11E–11F, Supplemental Figure 12E–12G and see Methods for details). All of these observations strongly support that FMO2 is a common regulator of tissue fibrosis with anti-fibrosis activity across different organs.

Discussion

Cardiac fibrosis following injury, especially secondary to MI, is a well-recognized detrimental factor in organ failure, including chronic heart failure. Although TGF-β signaling is an established pivotal pathway in fibroblast activation and cardiac fibrosis, there is still no clinically validated approach to treat fibrotic remodeling by blocking TGF-β signaling, and cardiac fibrosis remains one of the most challenging unmet clinic need with no effective therapies [20]. By interrogating the transcriptomic changes in post-MI hearts, we have discovered that the expression of a member of the Flavin Containing Monooxygenase (FMO) gene family, FMO2, is highly enriched in cardiac fibroblast and dynamically correlated with the onset of cardiac injury and fibrotic remodeling. Importantly, loss of FMO2 expression in fibroblasts is a conserved molecular signature in response to injury and TGF-β stimulation across different species from rodents to human, and FMO2 inactivation is sufficient to promote fibrotic induction and cardiac dysfunction. On the other hand, FMO2 expression effectively blocks TGF-β induced SMAD2/3 activation and fibroblast activation *in vitro*, and fibroblast specific FMO2 gene transfer effectively ameliorates cardiac fibrosis and dysfunction after myocardial infarction. The translational relevance of this finding is further supported by the *in vivo* evidence of FMO2 mediated cardiac protection against post-MI fibrotic remodeling in non-human primates and the *in vitro* results of FMO2 mediated inhibition of TGF-β signaling and myofibrotic activation in human fibroblasts from post-MI patients. Therefore, FMO2 is a previously uncharacterized regulator of TGF-β signaling with a conserved pivotal role in fibroblast activation and post-injury fibrotic remodeling.

The canonical function of most FMO gene family members [21] involves enzymatic activity-dependent cellular detoxifications [22]. Unexpectedly, however, the FMO2 mediated suppression of TGF-β activity is independent of its enzymatic activity. While non-enzymatic FMO2 isoforms have been reported in human and rat [18,23,24] and shows an effect on life span in *c.elegans* [25], its biological role has never been clearly elucidated. Our finding reveals for the first time an noncanonical and enzyme activity independent role of FMO2 in TGF-β signal transduction. Through unbiased proteomic analysis, we have identified CYP2J3 as a specific FMO2 binding protein necessary for downstream TGF-β regulation. CYP2J3 is a member of the cytochrome P450 superfamily which is largely known for oxidation of endogenous arachidonic acid pools as demonstrated previously in ischemic cardiomyocytes [26]. The human homolog of CYP2J3 (CYP2J2) is also reported to regulate cardiac

hypertrophy by suppressing phosphorylated SMAD3 via EET-11,12 secretion, a metabolite of arachidonic acids [27]. However, our data indicates that CYP2J3 also functions as a binding partner of FMO2 in TGF-β signal regulation. Furthermore, the FMO2-CYP2J3 interaction promotes the induction and nucleus translocation of SMURF2, an E3 ubiquitin ligase with specific activity towards phosphorylated SMAD2/3 in nucleus [19,28,29]. Therefore, our study has uncovered new non-canonical functions of FMO2 and CYP2J3, not as metabolic enzymes but as signaling modulators in a FMO2-CYP2J3-SMURF2 mediated negative regulatory circuit in TGF-β signaling towards SMAD2/3 phosphorylation and downstream gene activation in fibroblasts.

One of the major challenges in the current development of anti-fibrotic therapies (eg. targeting to TGF-β signaling or BMP signaling) is that the proof-of-concept evidence often come from small animal models, such as mouse and rat, rather than large animal species closer to human. Direct demonstration for the therapeutic prospect in large animals, especially in non-human primates, is rarely performed. In this study, we demonstrate that FMO2 expression in response to cardiac injury is conserved across multiple species, including mouse, rat, non-human primate and human. More importantly, we have directly tested the therapeutic effect of FMO2 expression in the post-injured hearts in monkeys. Thus, the findings from this study provide strong evidence in support of the prospect of translating this new strategy into a potential therapy to treat post-injured heart.

This finding also raises several new and important questions for future investigations. First, while FMO2 expression is dynamically regulated in response to TGF-β signaling activation or ischemic stress across multiple species, the underlying regulatory mechanism still needs to be elucidated. Further studies are needed to uncover the upstream molecular events leading to FMO2 down-regulation. Secondly, FMO2 expression in the disease models was accomplished using a lentiviral vector which has limitations in clinical application due to potential off-target side-effects, delivery technology and safety considerations. Therefore, an optimized delivery method, such as targeted delivery of a recombinant FMO2 protein or a smaller peptide, may need to be developed to make the therapeutic application practical in a clinical setting. Thirdly, previous study of CYP2J2, which is a functional homolog of human CYP2J3, shows that its cardioprotective effect is predominantly mediated by its metabolic products, 11,12 EET and subsequent activation of PPAR-γ signaling[27]. Hence, whether the enzymatic activity of CYP2J3 also contributes to FMO2 mediated anti-fibrosis effect needs to be investigated further. However, our data showed overexpression of CYP2J3 alone was not adequate to inhibit fibrotic induction which would argue against an enzyme dependent contribution from CYP2J3 without interacting with FMO2. Fourthly, we have uncovered a molecular target downstream of FMO2 in TGF-β regulation and SMAD2/3 phosphorylation is SMURF2. However, other downstream molecules may also be involved in FMO2 mediated regulation and remain to be fully characterized. Last but not least, although we used standardized criteria to analyze all database (eg. bulk RNA seq and single-nuclear RNA seq), while no appropriate tests were conducted to correct for multiple testing among gene databases.

Our major issues in the current development of anti-fibrotic therapies is that the proof-of-concept evidences often come from small animal models, such as mouse and rat, rather than

species close to human. Direct demonstration for the therapeutic prospect in large animals, especially in non-human primates, is rarely performed. In this study, we demonstrated that the loss of FMO2 expression in response to cardiac injury was a conserved molecular event across multiple species, including mouse, rat, monkey and human. More importantly, we have directly tested the therapeutic effect of FMO2 expression in the post-injured hearts in monkeys. These proof-concept evidence from a clinically relevant disease model support FMO2 as a novel negative regulator of TGF-β signaling and potential therapeutic strategy to exert potent anti-fibrotic function in heart across different species. Finally, as FMO2 and its interacting partners in TGF-β regulation are broadly expressed in different organs, our preliminary evidence from kidney also suggest that FMO2 expression has a potent protective effect against renal fibrosis post-injury, FMO2 mediated fibrotic regulation may have significant therapeutic implications beyond heart.

Supplementary Material

Refer to Web version on PubMed Central for supplementary material.

Acknowledgments

We thank all of the participants in the study and our colleagues, who contributed to data collection and sample dealing.

Source of Funding:

This work was supported by grants from National Key Research and Development Program of China (No. 2017YFA 0103700 for X. Hu; No. 2016YFC1301204 for J. Wang), National Natural Science Foundation of China (No. 81500176 for Y. Xu, No.81900328 for C. Ni, No.81320108003 and 31371498 for J. Wang; No. 81370247, 81622006, and 81670261 for X. Hu), the Fellowship of China Postdoctoral Science Foundation (No. 2020T130587 and No. 2019M652120 for C. Ni) and the Fundamental Research Funds for the Central Universities (No. LQ16H020003 for Y. Xu and No. 2019FZA7007 for C. Ni).

Nonstandard Abbreviations and Acronyms:

CF	Cardiac fibroblasts
EF	Ejection fraction
FS	Fraction shortening
LVIDs	Left Ventricular Internal Dimension (systolic)
LVIDd	Left Ventricular Internal Dimension (diastolic)
FMO2	Flavin Containing Monooxygenase 2
MI	Myocardial infarction
TGF-β	Transforming Growth Factor Beta
SMURF2	SMAD Ubiquitination Regulatory Factor 2
CYP2J3	Cytochrome P450 Superfamily 2J3
NHP	Non-human primate

ECM Extracellular Matrix

References

1. Cohn JN, Ferrari R, Sharpe N. Cardiac remodeling--concepts and clinical implications: a consensus paper from an international forum on cardiac remodeling. Behalf of an International Forum on Cardiac Remodeling. J Am Coll Cardiol. 2000;35:569–582. [PubMed: 10716457]
2. Tallquist MD, Molkentin JD. Redefining the identity of cardiac fibroblasts. Nature Reviews Cardiology. 2017;14:484–491. doi: 10.1038/nrcardio.2017.57 [PubMed: 28436487]
3. Mora AL, Rojas M, Pardo A, Selman M. Emerging therapies for idiopathic pulmonary fibrosis, a progressive age-related disease. Nat Rev Drug Discov. 2017;16:810. doi: 10.1038/nrd.2017.225
4. Humphreys BD. Mechanisms of Renal Fibrosis. Annu Rev Physiol. 2018;80:309–326. doi: 10.1146/annurev-physiol-022516-034227 [PubMed: 29068765]
5. Willyard C. Unlocking the secrets of scar-free skin healing. Nature. 2018;563:S86–S88. doi: 10.1038/d41586-018-07430-w [PubMed: 30464288]
6. Frangogiannis NG. Transforming growth factor-beta in myocardial disease. Nat Rev Cardiol. 2022. doi: 10.1038/s41569-021-00646-w
7. Frangogiannis NG, Kovacic JC. Extracellular Matrix in Ischemic Heart Disease, Part 4/4: JACC Focus Seminar. J Am Coll Cardiol. 2020;75:2219–2235. doi: 10.1016/j.jacc.2020.03.020 [PubMed: 32354387]
8. Moore-Morris T, Guimaraes-Camboa N, Yutzey KE, Puceat M, Evans SM. Cardiac fibroblasts: from development to heart failure. J Mol Med (Berl). 2015;93:823–830. doi: 10.1007/s00109-015-1314-y [PubMed: 26169532]
9. van den Borne SW, Diez J, Blankesteijn WM, Verjans J, Hofstra L, Narula J. Myocardial remodeling after infarction: the role of myofibroblasts. Nat Rev Cardiol. 2010;7:30–37. doi: 10.1038/nrcardio.2009.199 [PubMed: 19949426]
10. Novitskaya T, Chepurko E, Covarrubias R, Novitskiy S, Ryzhov SV, Feoktistov I, Gumina RJ. Extracellular nucleotide regulation and signaling in cardiac fibrosis. J Mol Cell Cardiol. 2016;93:47–56. doi: 10.1016/j.yjmcc.2016.02.010 [PubMed: 26891859]
11. Bujak M, Frangogiannis NG. The role of TGF-beta signaling in myocardial infarction and cardiac remodeling. Cardiovasc Res. 2007;74:184–195. doi: 10.1016/j.cardiores.2006.10.002 [PubMed: 17109837]
12. Dobaczewski M, Bujak M, Li N, Gonzalez-Quesada C, Mendoza LH, Wang XF, Frangogiannis NG. Smad3 signaling critically regulates fibroblast phenotype and function in healing myocardial infarction. Circ Res. 2010;107:418–428. doi: 10.1161/CIRCRESAHA.109.216101 [PubMed: 20522804]
13. Li RK, Li G, Mickle DA, Weisel RD, Merante F, Luss H, Rao V, Christakis GT, Williams WG. Overexpression of transforming growth factor-beta1 and insulin-like growth factor-I in patients with idiopathic hypertrophic cardiomyopathy. Circulation. 1997;96:874–881. [PubMed: 9264495]
14. Fan D, Takawale A, Lee J, Kassiri Z. Cardiac fibroblasts, fibrosis and extracellular matrix remodeling in heart disease. Fibrogenesis Tissue Repair. 2012;5:15. doi: 10.1186/1755-1536-5-15 [PubMed: 22943504]
15. Weber KT, Sun Y, Bhattacharya SK, Ahokas RA, Gerling IC. Myofibroblast-mediated mechanisms of pathological remodelling of the heart. Nat Rev Cardiol. 2013;10:15–26. doi: 10.1038/nrcardio.2012.158 [PubMed: 23207731]
16. Gonzalez A, Ravassa S, Beaumont J, Lopez B, Diez J. New targets to treat the structural remodeling of the myocardium. J Am Coll Cardiol. 2011;58:1833–1843. doi: 10.1016/j.jacc.2011.06.058 [PubMed: 22018293]
17. Li Y, Li Z, Zhang C, Li P, Wu Y, Wang C, Bond Lau W, Ma X-l, Du J. Cardiac Fibroblast–Specific Activating Transcription Factor 3 Protects Against Heart Failure by Suppressing MAP2K3-p38 Signaling. Circulation. 2017;135:2041–2057. doi: 10.1161/circulationaha.116.024599 [PubMed: 28249877]
18. Dolphin CT, Beckett DJ, Janmohamed A, Cullingford TE, Smith RL, Shephard EA, Phillips IR. The flavin-containing monooxygenase 2 gene (FMO2) of humans, but not of other primates,

encodes a truncated, nonfunctional protein. J Biol Chem. 1998;273:30599–30607. [PubMed: 9804831]

19. Lin X, Liang M, Feng X-H. Smurf2 Is a Ubiquitin E3 Ligase Mediating Proteasome-dependent Degradation of Smad2 in Transforming Growth Factor-β Signaling. Journal of Biological Chemistry. 2000;275:36818–36822. doi: 10.1074/jbc.C000580200 [PubMed: 11016919]
20. Kong P, Christia P, Frangogiannis NG. The pathogenesis of cardiac fibrosis. Cell Mol Life Sci. 2014;71:549–574. doi: 10.1007/s00018-013-1349-6 [PubMed: 23649149]
21. Dolphin CT, Shephard EA, Povey S, Smith RL, Phillips IR. Cloning, primary sequence and chromosomal localization of human FMO2, a new member of the flavin-containing mono-oxygenase family. Biochem J. 1992;287 (Pt 1):261–267. [PubMed: 1417778]
22. Siddens LK, Henderson MC, Vandyke JE, Williams DE, Krueger SK. Characterization of mouse flavin-containing monooxygenase transcript levels in lung and liver, and activity of expressed isoforms. Biochem Pharmacol. 2008;75:570–579. doi: 10.1016/j.bcp.2007.09.006 [PubMed: 17942081]
23. Whetstine JR, Yueh MF, McCarver DG, Williams DE, Park CS, Kang JH, Cha YN, Dolphin CT, Shephard EA, Phillips IR, et al. Ethnic differences in human flavin-containing monooxygenase 2 (FMO2) polymorphisms: detection of expressed protein in African-Americans. Toxicol Appl Pharmacol. 2000;168:216–224. doi: 10.1006/taap.2000.9050 [PubMed: 11042094]
24. Hugonnard M, Benoit E, Longin-Sauvageon C, Lattard V. Identification and characterization of the FMO2 gene in Rattus norvegicus: a good model to study metabolic and toxicological consequences of the FMO2 polymorphism. Pharmacogenetics. 2004;14:647–655. [PubMed: 15454729]
25. Leiser SF, Miller H, Rossner R, Fletcher M, Leonard A, Primitivo M, Rintala N, Ramos FJ, Miller DL, Kaeberlein M. Cell nonautonomous activation of flavin-containing monooxygenase promotes longevity and health span. Science. 2015;350:1375–1378. doi: 10.1126/science.aac9257 [PubMed: 26586189]
26. Wu S, Chen W, Murphy E, Gabel S, Tomer KB, Foley J, Steenbergen C, Falck JR, Moomaw CR, Zeldin DC. Molecular cloning, expression, and functional significance of a cytochrome P450 highly expressed in rat heart myocytes. J Biol Chem. 1997;272:12551–12559. doi: 10.1074/jbc.272.19.12551 [PubMed: 9139707]
27. He Z, Zhang X, Chen C, Wen Z, Hoopes SL, Zeldin DC, Wang DW. Cardiomyocyte-specific expression of CYP2J2 prevents development of cardiac remodelling induced by angiotensin II. Cardiovasc Res. 2015;105:304–317. doi: 10.1093/cvr/cvv018 [PubMed: 25618409]
28. Zhang L, Zhou F, Garcia de Vinuesa A, de Kruijf EM, Mesker WE, Hui L, Drabsch Y, Li Y, Bauer A, Rousseau A, et al. TRAF4 promotes TGF-beta receptor signaling and drives breast cancer metastasis. Mol Cell. 2013;51:559–572. doi: 10.1016/j.molcel.2013.07.014 [PubMed: 23973329]
29. Zhang Z, Fan Y, Xie F, Zhou H, Jin K, Shao L, Shi W, Fang P, Yang B, van Dam H, et al. Breast cancer metastasis suppressor OTUD1 deubiquitinates SMAD7. Nat Commun. 2017;8:2116. doi: 10.1038/s41467-017-02029-7 [PubMed: 29235476]
30. Bergmann O, Jovinge S. Isolation of cardiomyocyte nuclei from post-mortem tissue. J Vis Exp. 2012. doi: 10.3791/4205
31. Yokota T, McCourt J, Ma F, Ren S, Li S, Kim TH, Kurmangaliyev YZ, Nasiri R, Ahadian S, Nguyen T, et al. Type V Collagen in Scar Tissue Regulates the Size of Scar after Heart Injury. Cell. 2020;182:545–562 e523. doi: 10.1016/j.cell.2020.06.030 [PubMed: 32621799]
32. Stuart T, Butler A, Hoffman P, Hafemeister C, Papalexi E, Mauck WM, 3rd, Hao Y, Stoeckius M, Smibert P, Satija R. Comprehensive Integration of Single-Cell Data. Cell. 2019;177:1888–1902 e1821. doi: 10.1016/j.cell.2019.05.031 [PubMed: 31178118]
33. Butler A, Hoffman P, Smibert P, Papalexi E, Satija R. Integrating single-cell transcriptomic data across different conditions, technologies, and species. Nature biotechnology. 2018;36:411-+. doi: 10.1038/nbt.4096
34. van Rooij E, Fielitz J, Sutherland LB, Thijssen VL, Crijns HJ, Dimaio MJ, Shelton J, De Windt LJ, Hill JA, Olson EN. Myocyte enhancer factor 2 and class II histone deacetylases control a gender-specific pathway of cardioprotection mediated by the estrogen receptor. Circ Res. 2010;106:155–165. doi: 10.1161/CIRCRESAHA.109.207084 [PubMed: 19893013]

35. Lin J, Steenbergen C, Murphy E, Sun J. Estrogen receptor-beta activation results in S-nitrosylation of proteins involved in cardioprotection. Circulation. 2009;120:245–254. doi: 10.1161/CIRCULATIONAHA.109.868729 [PubMed: 19581491]

36. Hamada H, Kim MK, Iwakura A, Ii M, Thorne T, Qin G, Asai J, Tsutsumi Y, Sekiguchi H, Silver M, et al. Estrogen receptors alpha and beta mediate contribution of bone marrow-derived endothelial progenitor cells to functional recovery after myocardial infarction. Circulation. 2006;114:2261–2270. [PubMed: 17088460]

37. Rossouw JE. Estrogens for prevention of coronary heart disease. Putting the brakes on the bandwagon. Circulation. 1996;94:2982–2985. [PubMed: 8941130]

38. Stampfer MJ, Willett WC, Colditz GA, Rosner B, Speizer FE, Hennekens CH. A prospective study of postmenopausal estrogen therapy and coronary heart disease. N Engl J Med. 1985;313:1044–1049. [PubMed: 4047106]

39. Wang P, Luo ML, Song E, Zhou Z, Ma T, Wang J, Jia N, Wang G, Nie S, Liu Y, et al. Long noncoding RNA lnc-TSI inhibits renal fibrogenesis by negatively regulating the TGF-beta/Smad3 pathway. Sci Transl Med. 2018;10. doi: 10.1126/scitranslmed.aat2039

Novelty and Significance

What Is Known?

- Cardiac fibrosis is a severe adverse long-term pathophysiology process in ischemic heart diseases, which leads to heart failure and malignant arrythmia with no effective remedy.
- Flavin containing monooxygenase 2 (FMO2) is one of the FMO family known for its NADH/FAD dependent enzymatic bioactivity, with little known of its function in cardiac diseases.
- Phosphorylated SMAD2/3 plays significant role in mediating cardiac fibrosis triggered by Transforming growth factor β (TGF-β) secretion post myocardial infarction (MI).

What New Information Does This Article Contribute?

- We discovered significant down-regulation of Flavin containing monooxygenase 2 (FMO2) in heart, especially in cardiac fibroblasts, subsequent to myocardial infarction (MI).
- FMO2 genetic ablation incurs significantly augmented cardiac fibrosis accompanied by impaired cardiac function, whereas the restoration of FMO2 expression reversed excessive cardiac fibrosis as well as rescued cardiac function from rodents to non-human primates.
- FMO2-cytochrome p450 superfamily 2J3 (CYP2J3)-SMAD specific ubiquitination E3 ligase 2 (SMURF2)-pSMAD2/3 axis plays important roles in cardiac remodeling under ischemic condition downstream of TGF- β signaling. FMO2 acts as a “leverage” in controlling phosphorylation levels of SMAD2/3, and thus regulates cardiac fibrosis and maintains the homeostasis of cardiac fibroblasts.

Cardiac fibrosis is a severe pathological feature associated with adverse clinical outcomes in post-injury remodeling with limited therapy. We identified FMO2 as one of the top-ranked genes suppressed after myocardial infarction (MI) from rodents to non-human primates. Genetic inactivation of FMO2 in rats markedly induced spontaneous cardiac fibrosis in heart and extended to lung and kidney. In fibroblasts, FMO2 expression potently inhibited TGF-β induced fibrotic activation and suppressed SMAD2/3 signaling by promoting nuclear translocation of SMURF2. However, FMO2 mediated regulation of SMURF2 required the interaction with CYP2J3. Significantly, ectopic expression of FMO2 specifically in cardiac fibroblast markedly reduced cardiac fibrosis in rodents with reinforced cardiac function post MI. Finally, we demonstrated a strong anti-fibrotic ability of FMO2 in post-MI non-human primates using lentiviral vector, leading to significantly improved cardiac function. Therefore, our study has uncovered a previously uncharacterized activity of FMO2 in fibrotic regulation and expression of FMO2 is a potential therapeutic modality for post-injury cardiac remodeling and also universally suitable in multiple organs under fibrotic circumstances.

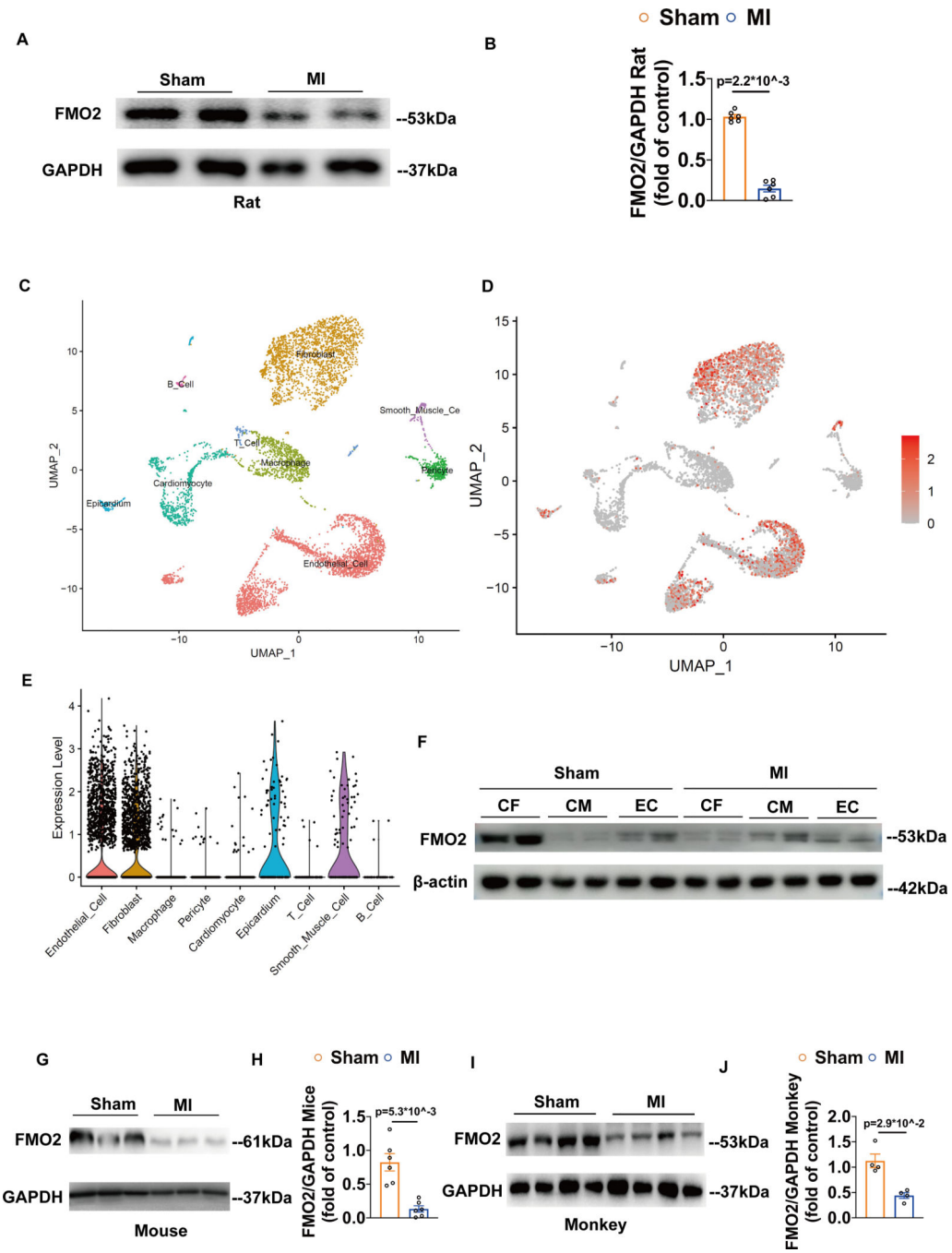

Figure 1. Myocardial injury triggers down-regulation of FMO2 (A-B).

FMO2 protein level in hearts (infarct zone) from post-MI SD rats (28 days post MI)**(A)** and quantitative analyses were plotted in **(B),** n=6 in each group; **(C)** UMAP plot showing 9 annotated cell types based on top enriched marker genes in the snRNA-seq data from 2 WT mouse hearts. **(D)** Feature Plot showing FMO2 scaled expression across the whole cell clusters in the dataset of **C)**. Red dots labeling cells expressing FMO2 with up to 95% of the maximum level, and the top 5% high expressing cells were filtered in case of any unknown bias. **(E)** Violine Plot showing FMO2 scaled expression across the whole cell

types in the mouse heart snRNA-seq data as shown in **D)**. Default settings was used for the function in Seurat. **(F)** Western blotting conducted on cardiac fibroblast, cardiomyocyte and endothelial cells respectively isolated from sham or MI rats' heart, FMO2 was determined to be mostly expressed in cardiac fibroblast in *ex vivo* heart. **(G-H)** Protein levels of FMO2 in hearts after myocardial infarction in mice with representative immunoblot images in **(G)** and quantitative analyses were plotted in (**H)**, n=6 in each group. **(I-J).** FMO2 expression in hearts harvested from post-MI monkeys, quantitative analyses were plotted in **(J)**, n=4 in each group. Student's tests were conducted in **(B), (H),** and Mann-Whitney test was utilized in **(J).**

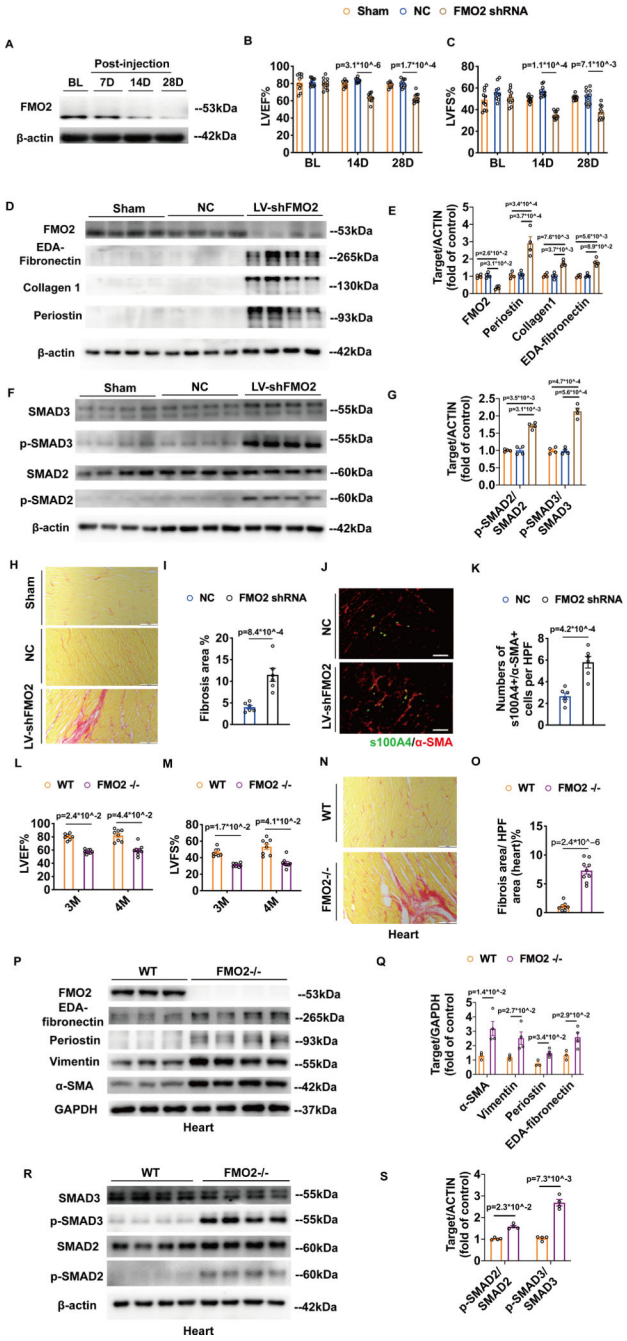

Figure 2. Loss of FMO2 incurs cardiac fibrosis accompanied by deteriorated cardiac function

(A). FMO2 protein level in rat heart at day 7, 14 and 28 after injection of the lentivial vector expressing FMO2 shRNA. **(B-C)**. Left ventricular ejection fraction **(B)**, left ventricular fraction shortening **(C)** measured by 2D echocardiography on rats received FMO2 shRNA and NC respectively at different time points (baseline, 14 and 28 days after injection), n=10 in each group. **(D-G)** Immunoblots for ECM proteins, including EDA-fibronectin, Collagen 1, periostin **(D)** as well as pro-fibrotic signaling (phosphorylated SMAD2/3) **(F)** in Sham, NC and LV-shFMO2 rat heart tissues **(E)** respectively. The summary data of were

shown in **(E)** and **(G)**, n=4 in each group, **(H)** Representative images of left ventricular stained with Sirius red showing degrees of fibrosis in rats treated with Sham, control (NC) and FMO2 shRNA vectors. (**I)** Quantitative summary of changes in fibrosis in the hearts treated with FMO2 shRNA compared with the rats treated with NC vectors, n=6 in each group, scale bar = 100μm. **(J)**. Immunofluorescence staining for α-smooth muscle actin (α-SMA)–positive (red) and s100A4 positive (green) cardiac fibroblasts, scale bar = 100μm. **(K)** Quantification of α-SMA-s100A4 double positive cells per field. n=6 in each group. **(L)** Left ventricle ejection fraction (LVEF) and **(M)** fractional shortening (LVFS) of WT and $FMO2^{-/-}$ rats at 12 and 16 week after birth, n=8 in WT group, n=9 in $FMO2^{-/-}$ group. Error bar is SEM. **(N)**. Picrosirius red staining showing different degrees of fibrosis in heart from WT and FMO2−/− rats. The summary data of fibrosis were shown in **(O)** for heart, n=8 in WT group, n=9 in $FMO2^{-/-}$ group, scale bar = 100μm. Error bar indicates SEM. **(P-Q)** Immunoblots for ECM proteins, including EDA-fibronectin, periostin, vimentin, and α-SMA, in WT (n=3) and FMO2−/− (n=4) rat heart tissues (**P)**. Quantitative analyses were plotted in (**Q). (R-S)** Immunoblots for phosphorylation SMAD2/3 in WT and FMO2−/− group respectively (**R)**. Quantitative analyses were plotted in (**S),** n=4 in each group. Two-way ANOVA followed by Sidak post hoc multiple comparisons test were conducted in **(B-C)**. Kruskal-Wallis followed by Dunn post hoc multiple comparisons test were conducted in **(E)** and **(G).** Student's tests were conducted in **(I), (K), (L), (M), (O).** Mann-Whitney test was utilized in **(Q)** and **(S).**

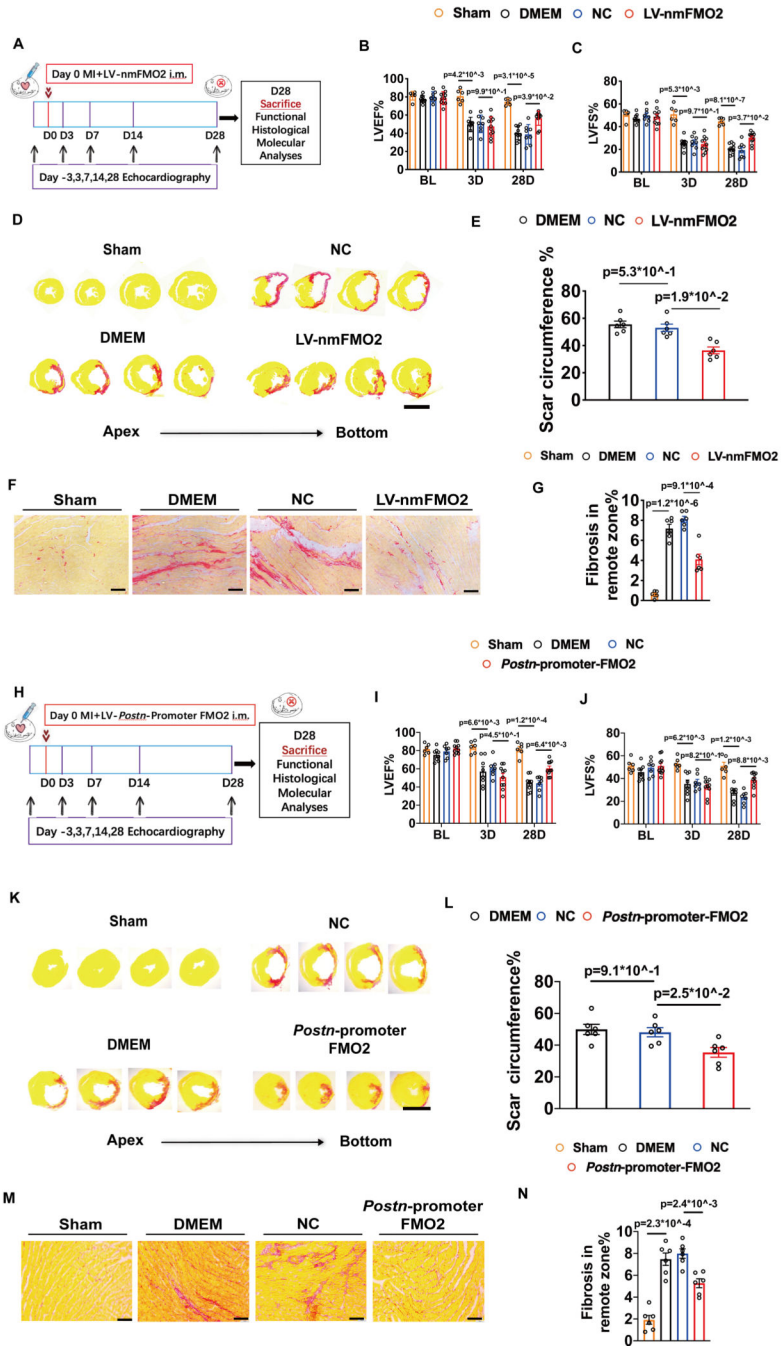

Figure 3. Therapeutic utilization of cardiac-fibroblast targeted FMO2 expression in ameliorating cardiac fibrosis after myocardial infarction

(A). Schematic experimental outline for intra-myocardial administration of non-myocyte targeted LV-FMO2 vector after MI surgery. **(B).** LVEF and **(C)** LVFS measured from 2-dimensional echocardiography in each experimental group including Sham, MI+DMEM, MI+NC, MI+miR133a/1a-TS-FMO2 (LV-nmFMO2), at different time points following MI, n=6 in sham and n=9 in MI+DMEM group, n=8 in MI+NC and n=11 in MI+LV-nmFMO2 group. **(D)** Representative images of picrosirius red staining from sequential heart sections

on rats from each experimental group. (**E**) summary data on scar sizes, n=6 in each group. Scale bar = 1 cm. **(F),** Representative images of interstitial fibrosis in non-infarcted areas in heart from each experimental group. **(G)**. Quantification of tissue fibrotic plotted as percent areas (means with SEM), n=6 per group. Scale bar = 100μm. **(H).** Schematic experimental outline for intra-myocardial administration of *Postn*-promoter FMO2 lentivirus following MI surgery. **(I).** LVEF and **(J)** LVFS measured from 2-dimensional echocardiography in each experimental group including Sham, MI+DMEM, MI+NC, *Postn*-promoter FMO2, at different time points following MI, n=6 in sham and n=8 in MI+DMEM group, n=7 in MI+NC and n=10 in *Postn*-promoter FMO2 group. **(K)** Representative images of picrosirius red staining from sequential heart section from rats of each experimental group. (**L**) Summary data of scar sizes, n=6 in each group. Scale bar = 1 cm. **(M),** Representative images of the interstitial fibrosis in non-infarcted area in each group. **(N)**. Quantification of fibrosis was plotted as percentage of fibrotic areas (means with SEM), n=6 per group. Scale bar = 100μm. Two-way ANOVA followed by Sidak post hoc multiple comparisons test were conducted in **(B-C)** and **(I-J).** One-way ANOVA followed by Tukey post hoc multiple comparisons test were conducted in **(E), (G), (L), (N).**

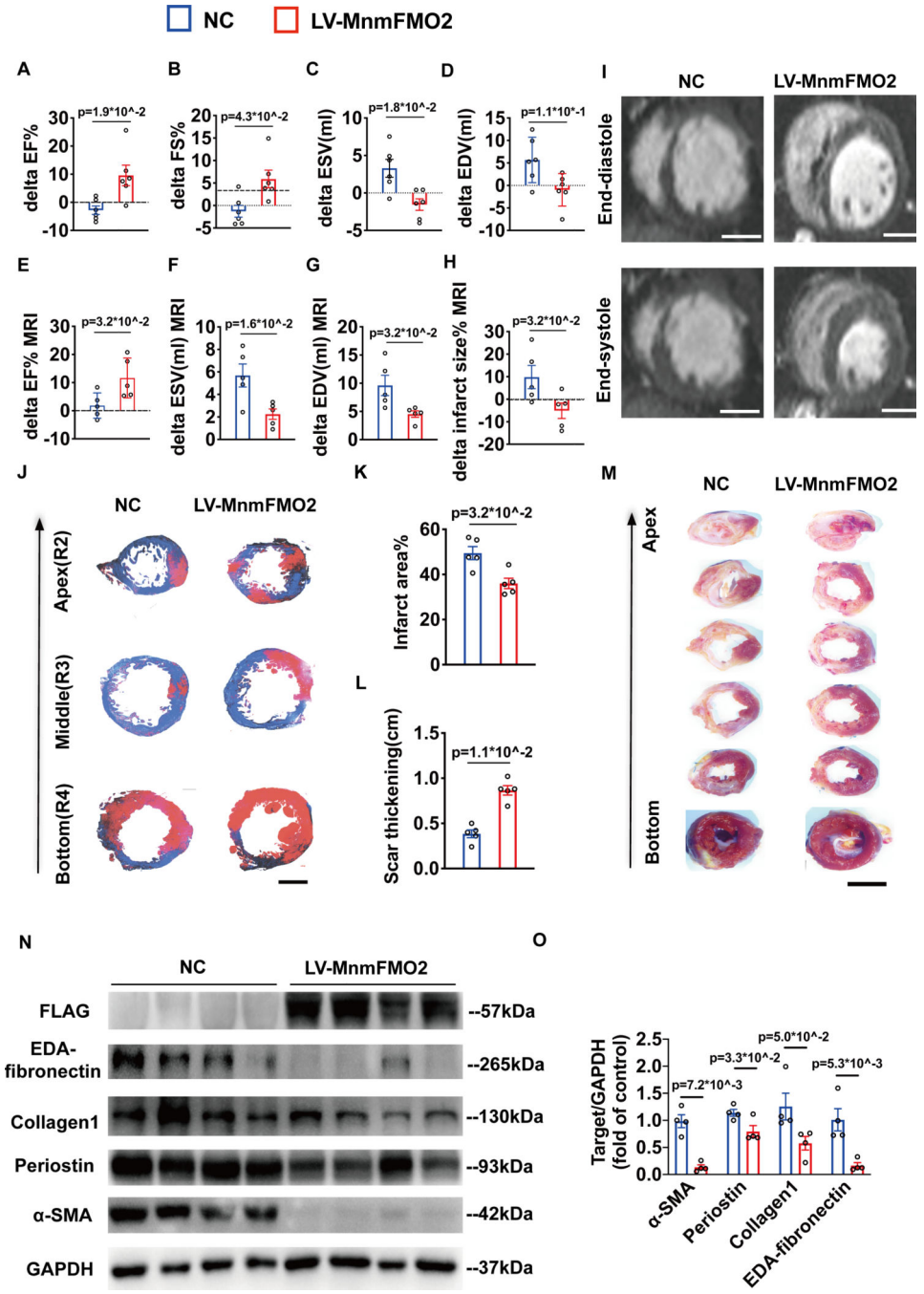

Figure 4. Targeted expression of FMO2 in non-human primate heart after myocardial infarction significantly improves heart function.

(A-D) Changes in echocardiographic parameters between day-3 and 1-month post-LAD ligation in monkeys treated with a control lentiviral vector (NC) or the lentiviral vector expressing monkey miR133a/1a-TS-FMO2 (LV-MnmFMO2), including **(A)** ejection fraction (EF), **(B)** fractional shortening (FS), **(C)** end systolic volume (ESV), and **(D)** end-diastolic volume (EDV), as indicated, n=6 each group. (**E-H**) Changes in cardiac parameters between day 3 and 1 month post-LAD ligation measured by MRI in monkeys treated with

a control lentiviral vector (NC) or the lentiviral vector expressing miR133a/1a-TS-FMO2 (LV-MnmFMO2), including **(E)** ejection fraction (EF), **(F)** end systolic volume (ESV), **(G)** end-diastolic volume (EDV), and **(H)** estimated infarct sizes as indicated, n=5 in each group. **(I)** Representative short-axis cine MRI images at end-diastolic and end-systolic phases of the cardiac cycle 1 month after MI. Scale bar = 1cm. **(J).** Representative images of MASSON trichrome staining on ventricular sections from monkeys treated with control vector (NC) and the lentiviral vector expressing miR133a/1a-TS-FMO2 (LV-MnmFMO2), scale bar = 1cm. Summary data of scar areas **(K**) and scar thickness **(L)**, n=5 in each group. **(M)** Representative consecutive segments sliced from monkey hearts one month after MI and treated with control vector (NC) and the lentiviral vector expressing miR133a/1a-TS-FMO2 (LV-MnmFMO2). Scale bar = 2cm. **(N-O)** Expression of extracellular matrix proteins in heart tissues harvested from monkey hearts. n=4 in each group as indicated, GAPDH was served as a loading control. Statistical analyses were plotted in (**O).** Student's tests were conducted in **(A-D),** Mann-Whitney test were utilized in **(E-H), (K-L)** and **(O).**

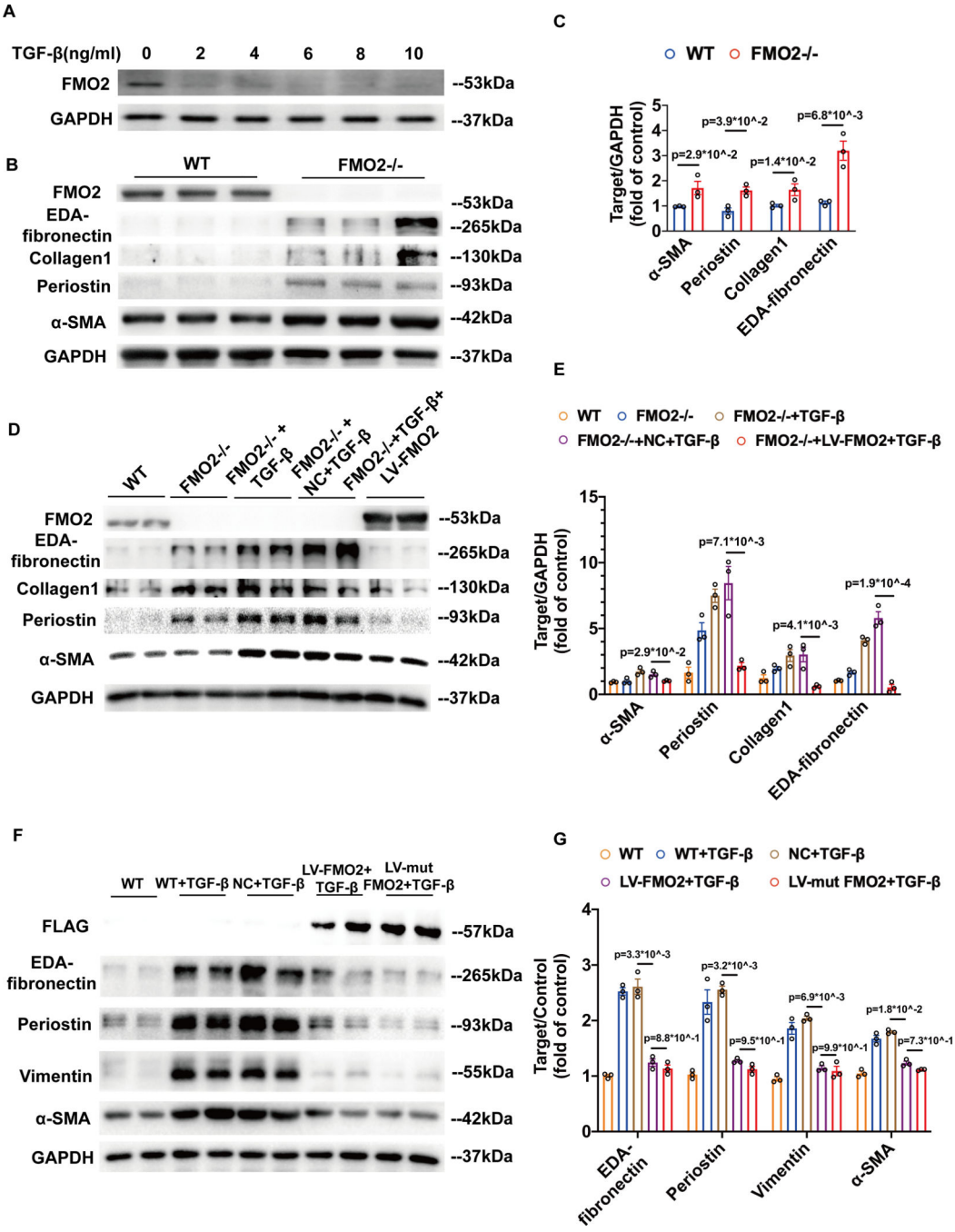

Figure 5. FMO2 exerts anti-fibrotic effect on TGF-β stimulated cardiac fibroblasts independent of its enzymatic activity.

(A). FMO2 protein detected in isolated neonatal cardiac fibroblast after TGF-β treatment at different concentration as indicated. **(B)** Fibrotic protein expression in cardiac fibroblasts (CF) isolated from WT adult rat heart or the $FMO2^{-/-}$ adult rat heart as indicated. **(C)** Quantitative bar graphs of fibrotic proteins, n=3 in each group. (**D**) Fibrotic protein expression in cardiac fibroblast isolated from $FMO2^{-/-}$ adult rat following TGF-β treatment with or without co-treatment of lenti-FMO2 (LV-FMO2) vector as labeled (**E)** Quantitative

of fibrotic proteins were plotted, n=3 in each group. (**F).** Fibrotic protein levels in the wildtype CFs (WT) treated without or with TGF-β plus LV-FMO2 or LV-mut FMO2 mutant as indicated. **(G)** Quantitative results of fibrotic proteins from (**F**) were plotted, n=3 in each group. Student's t test was utilized in **(C)**, One-way ANOVA followed by Tukey post hoc multiple comparisons test were conducted in **(E), (G).**

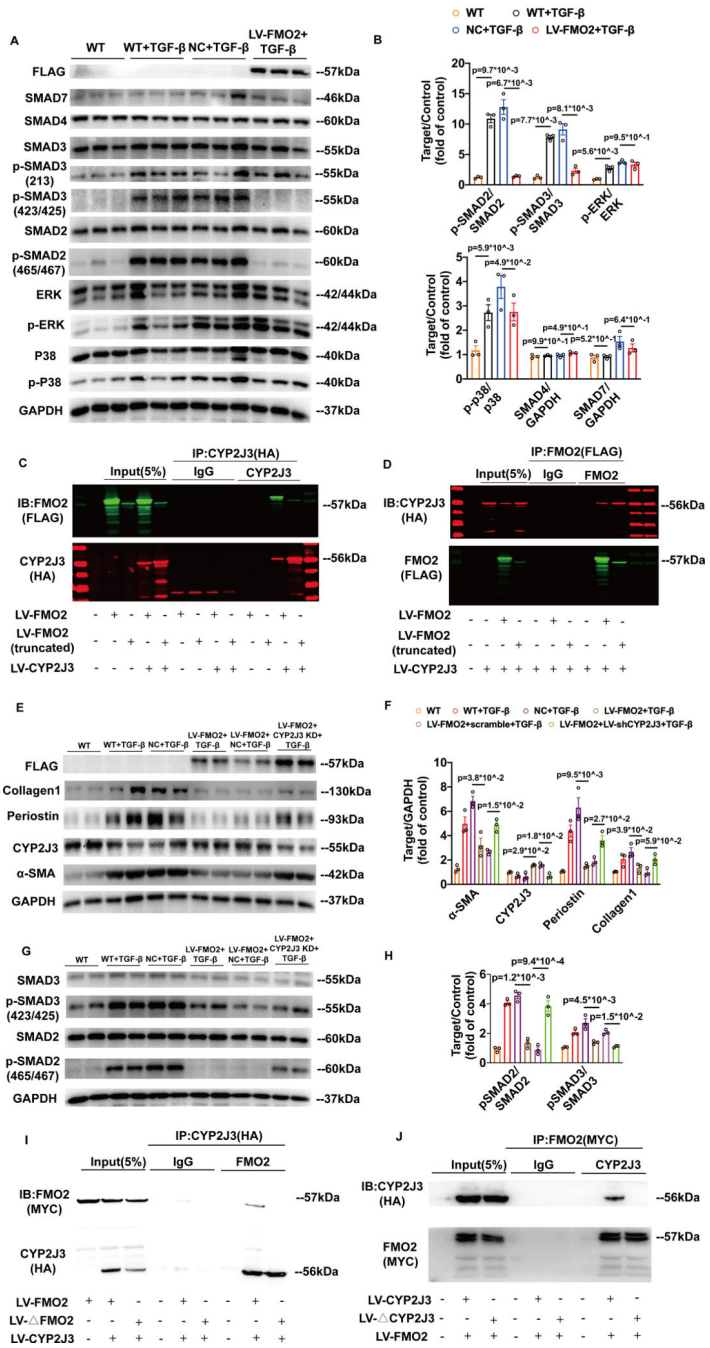

Figure 6. FMO2 inhibits phosphorylated SMAD2/3 via interaction with CYP2J3.

(A-B). TGF-β downstream signaling molecules detected by western blot in cardiac fibroblasts (CFs) in response to TGF-β stimulation with or without FMO2 expression, showing a specific impact on phosphor-SMAD2/3 levels. **A)**. Quantitative analyses were plotted in **B)**, n=3 in each group**. (C).** Co-immunoprecipitation assay showing FMO2-CYP2J3 binding in CFs expressing FLAG-FMO2 and HA-CYP2J3 using anti-HA for immunoprecipitation followed by anti-FLAG immunoblotting. **(D)** Co-immunoprecipitation assay in CFs expressing FLAG-FMO2 and HA-CYP2J3 using anti-

FLAG for immunoprecipitation followed by anti-HA immunoblotting. **(E-F).** Immunoblot of fibrotic proteins in TGF-β stimulated CFs with FMO2 expression and CYP2J3 knock-down by a lenti-vector (LV-shCYP2J3) as indicated **E),** Quantitative analyses were plotted in **F)**, n=3 in each group**. (G-H)** TGF-β signal and phosphorylation of SMAD2/3 in CFs treated with TGF-β and lentivectors for FMO2 (LV-FMO2) and CYP2J3 shRNA (LV-shCYP2J3) as indicated **G)**, Quantitative analyses were plotted in **H)**, n=3 in each group**. (I).** Co-immunoprecipitation assay using wildtype CYP2J3 and wildtype and mutated FMO2. **(J).** Co-immunoprecipitation assays using wildtype FMO2 with wildtype and mutated CYP2J3. One-way ANOVA followed by Tukey post hoc multiple comparisons test were conducted in **(B), (F), (H).**

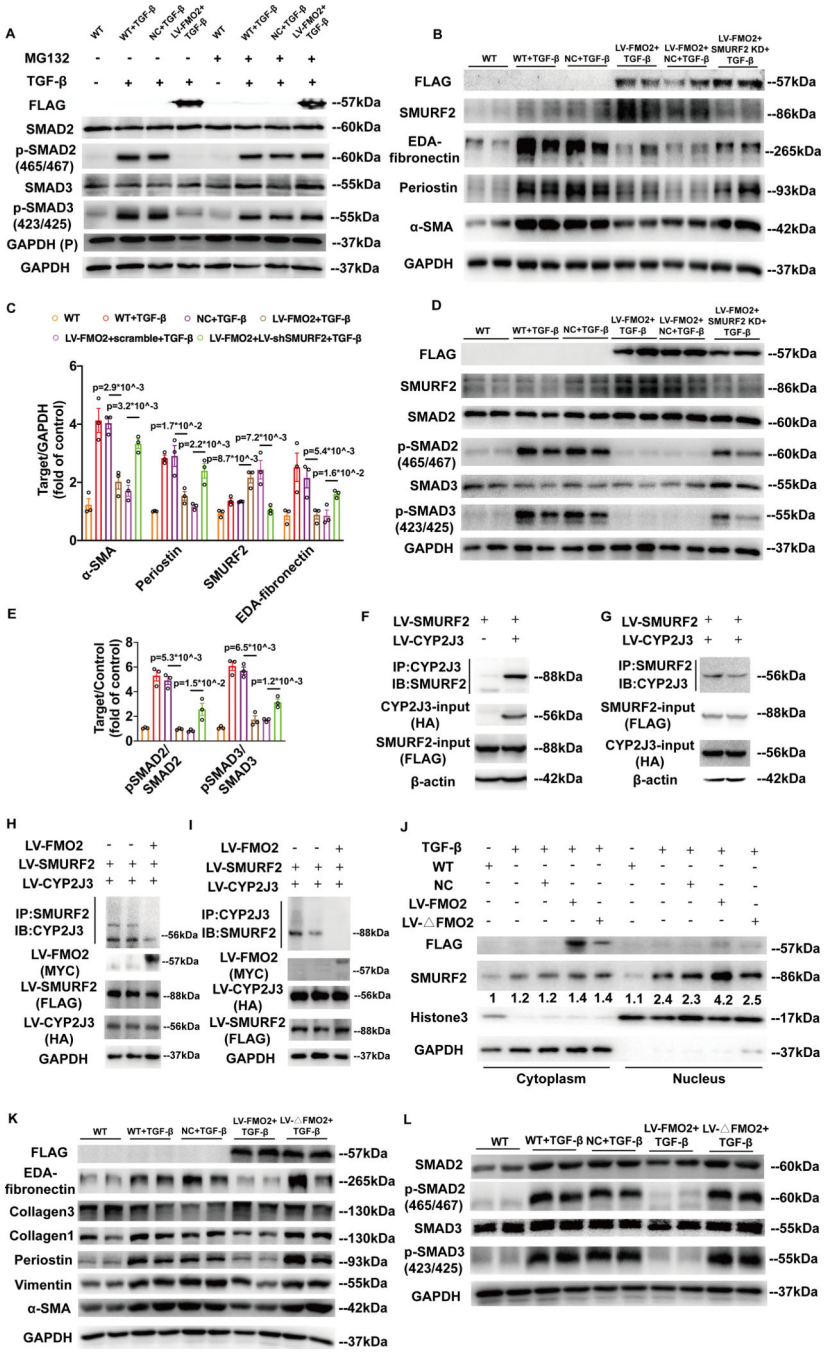

Figure 7. FMO2-CYP2J3 inhibits phosphorylation of SMAD2/3 via promoting SMURF2 nuclear translocation.

A). MG132 treatment in NRCF reversed the inhibition of phosphorylated SMAD2/3 exerted by FMO2 in the present of TGF-β stimulation. **(B-C).** Immunoblots display extracellular matrix protein synthesis in CFs treated with TGF-β, FMO2 overexpression, and SMURF2 knockdown (LV-shSMURF2) as indicated **B)**. Quantitative analyses were plotted in **C)**, n=3 in each group**. (D-E)**. Immunoblots showing phosphorylation of SMAD2/3 in CFs treated as in B. **D)** Quantitative analyses were plotted in **E)**, n=3 in each group. **(F-G).** Reciprocal co-

immunoprecipitation assays between CYP2J3 and SMURF2 in CFs expressing HA-CYP2J3 and FLAG-SMURF2. **(H-I).** FMO2 over-expression reduced interaction between CYP2J3 and SMURF2 **(J).** Increased nuclear translocation of SMURF2 was observed in CFs by FMO2 overexpression under TGF-β stimulation as shown in western blots from the cytosolic and the nuclear fractions as indicated. Fold change of SMURF2 in each group as compared with SMURF2 in cytoplasm of WT were annotated under the band, n=3 in each group. **(K-L).** Immunoblots displayed alterations of extracellular protein synthesis **(K)** and phosphorylation of SMAD2/3 **(L)** in NRCFs expressing wildtype FMO2 or CYP2J3 binding site mutated FMO2 (△FMO2). One-way ANOVA followed by Tukey post hoc multiple comparisons test were conducted in **(C), (E).**

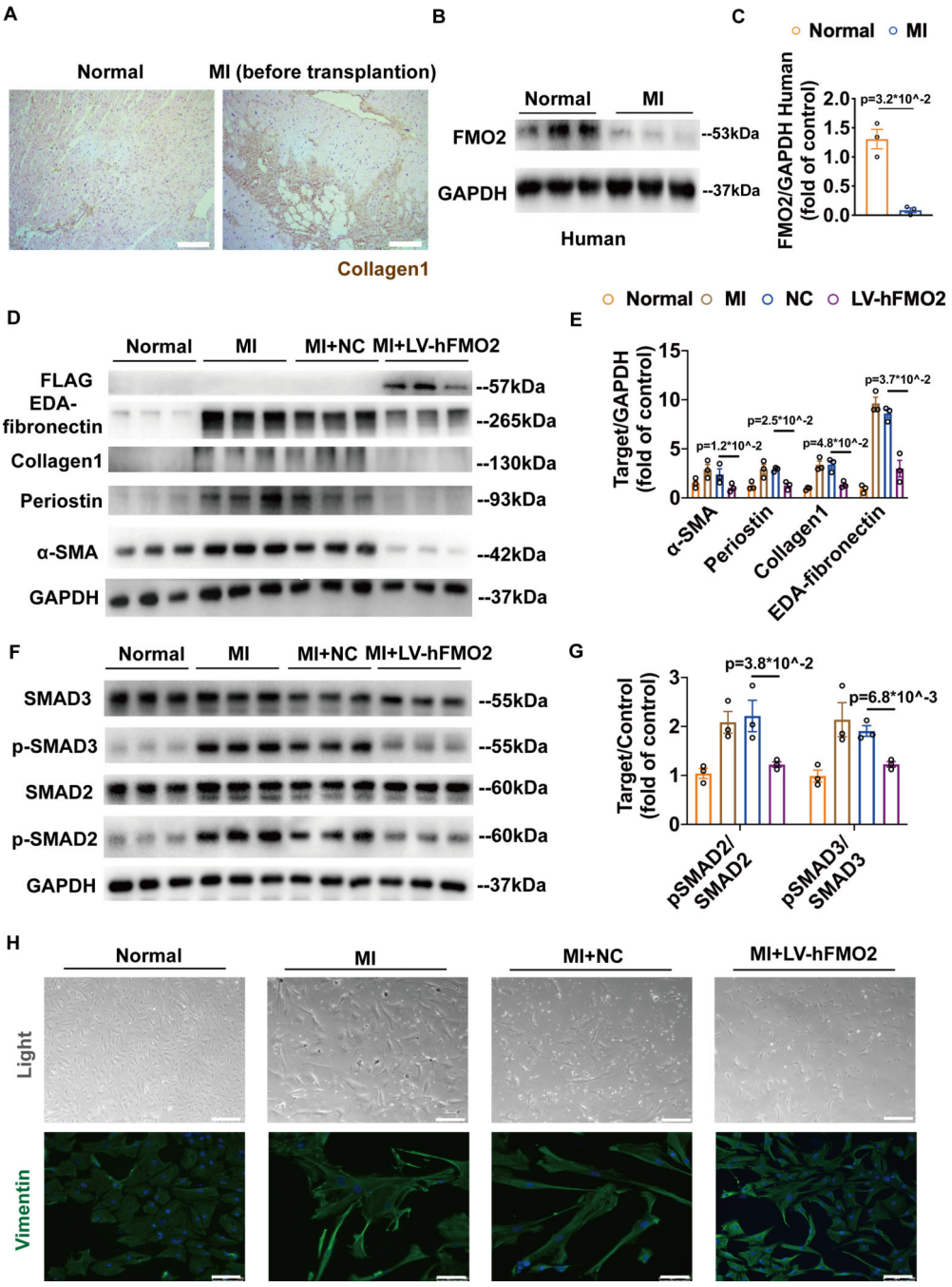

Figure 8. FMO2 expression and anti-fibrosis effect in human samples

A). Collagen1 staining in hearts from LV free wall of normal control and MI patients respectively. Scale bar = 100μm. **(B).** FMO2 expression in heart tissues from healthy controls and MI patients, n=3 in each group and (**C)** quantitative results**. (D).** Levels of extracellular matrix proteins in CF isolated from normal and post-MI human hearts, as well as CF from a MI heart transfected with lentiviral vectors for non-specific control (NC) and expressing human FMO2 (LV-hFMO2), and (**E)** quantitative results, n=3 in each group**. (F).** Levels of pro-fibrotic signaling in CF isolated from normal and post-MI human

hearts, as well as CF from a MI heart transfected with lentiviral vectors for non-specific control (NC) and expressing human FMO2 (LV-hFMO2), and (**G)** quantitative results, n=3 in each group. **(H).** Cellular morphology and vimentin expression profile observed using immunofluorescence staining in CFs from normal, MI, MI+NC, MI+LV-hFMO2, scale bar = 100μm in immunostaining images, scale bar = 250μm in light visions. One-way ANOVA followed by Tukey post hoc multiple comparisons test were conducted in **(E)** and **(G)**, Mann-Whitney test were utilized in **(C).**